Fast Diffusion of Br^- Ions on a Micellar Surface

N. Hedin and I. Furó*

Division of Physical Chemistry, Department of Chemistry, Royal Institute of Technology, SE-10044 Stockholm, Sweden

Received: May 24, 1999; In Final Form: September 3, 1999

An accurate determination of the field-dependent spin relaxation rates of ^{81}Br by NMR provides, through the motional correlation time, the lateral surface diffusion coefficient of the Br^- ions that are electrostatically confined to the vicinity of the oppositely charged surface of $C_{16}TABr$ micelles. We find that the Br^- counterions diffuse about 1 order of magnitude faster than the $C_{16}TA^+$ molecules. The obtained diffusion coefficient is about 10^{-9} m^2/s, roughly half the bulk diffusion coefficient of Br^-. The residual quadrupole coupling constant is small, around 1 MHz, indicating a high symmetry for the Br^- environment on the $\geq$100 ps time scale.

Introduction

The state of counterions,[1] condensed in the vicinity of the oppositely charged surface of micelles, has been the subject of numerous studies. Among these, NMR experiments have been particularly useful for clarifying the general picture. By the study of the NMR spin relaxation of counterions, in most cases with $I > 1$ spins, which dominantly relax via their quadrupolar coupling, the following consensus[2−4] has appeared. (i) The micellar surface causes a slight average deformation of the hydration shell of the counterions compared to that in a dilute solution. This deformation causes the electric quadrupole coupling, which is averaged to zero by fast ($\sim$ picosecond) motions in the dilute solution case, to remain nonzero on the time scale of $\sim$100 ps. (ii) The characteristic direction of this residual coupling coincides with the local surface normal of the micelle. (iii) In isotropic systems such as micellar solutions, the residual quadrupole coupling is further averaged to zero by two orientational averaging processes: ion diffusion on the micellar surface[5−7] and isotropic tumbling of the aggregates. This dynamical step, if suitably placed compared to the NMR frequencies, provides a clear NMR fingerprint: a frequency-dependent spin relaxation[8,9] that scales as expected from the geometrical parameters.[10,11] As has been shown for Na^+ ions, the lateral ion mobility is reduced with respect to to its value in bulk solutions as an effect of the headgroups.[10,12]

The present study is motivated from three directions. First, Br^- ions are still (despite a clear exposition of the contrary[13−15]) often described or indicated as "bound" to the micellar surface, where a "bound" ion seems to be pictured as specifically attached via an unclear mechanism to (some site of) the headgroup. Such pictures emerge more frequently for Br^- because of the large ion effect exhibited when changing to this counterion. Second, while the state of positively charged alkali counterions has already been investigated,[10,12] there is no corresponding NMR data for the negatively charged and more polarizable halide ions. The results we present below for Br^- are in many respects similar to those obtained for Na^+ counterions: the Br^- ions are far from being immobilized and diffuse considerably more quickly than the corresponding surfactant molecules. Finally, strong counterion effects on the micellar structure are experienced when replacing Br^- by Cl^- ions;[16,17] managing an NMR spin relaxation study on the technically more demanding bromine opens the door to a comparative study of those two counterions. On the other hand, our findings might also prove helpful when analyzing findings from other areas such as neutron reflection,[18,19] counterion competition,[20,21] molecular dynamics simulation,[22−24] and preparation of mesoporous materials by counterion polymerization on surfactant templates.[25]

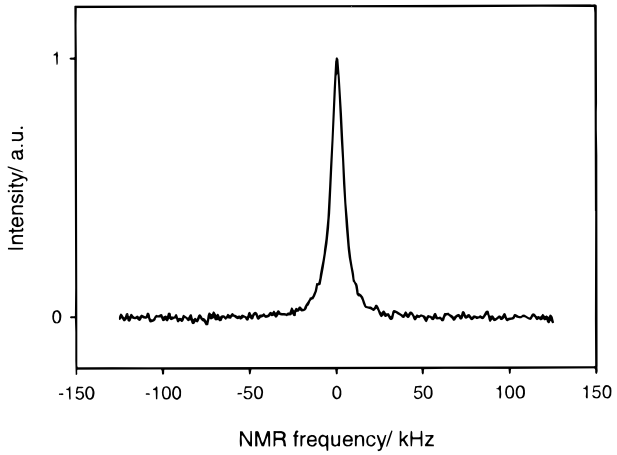

Figure 1. ^{81}Br NMR spectrum of a micellar solution of hexadecyltrimethylammonium bromide ($C_{16}TABr$) at 54 MHz. Spectral distortion due to ringing is reduced by using a composite pulse (see text) for recording the signal.

Experimental Section

A sample of 0.10 M (=3.64 wt %) surfactant concentration has been produced by mixing hexadecyltrimethylammonium bromide ($C_{16}TABr$, often also called as CTAB) and Millipore filtered water. The selected concentration is the same as in a related work where the micellar shape is investigated by ^2H NMR relaxation.[26] The ^{81}Br NMR measurements were performed on Bruker DMX500 (with the Larmor frequency $\omega_0/(2\pi) = 135$ MHz for ^{81}Br), AMX300 (81 MHz), and DMX200 (54 MHz, spectrum shown in Figure 1) spectrometers equipped with superconducting magnets and with a field-variable

* To whom correspondence should be addressed. Phone: +46 8 7908592. Fax: +46 8 7908207. E-mail: ifuro@physchem.kth.se.

10.1021/jp991687g CCC: $18.00
Published on Web 10/15/1999

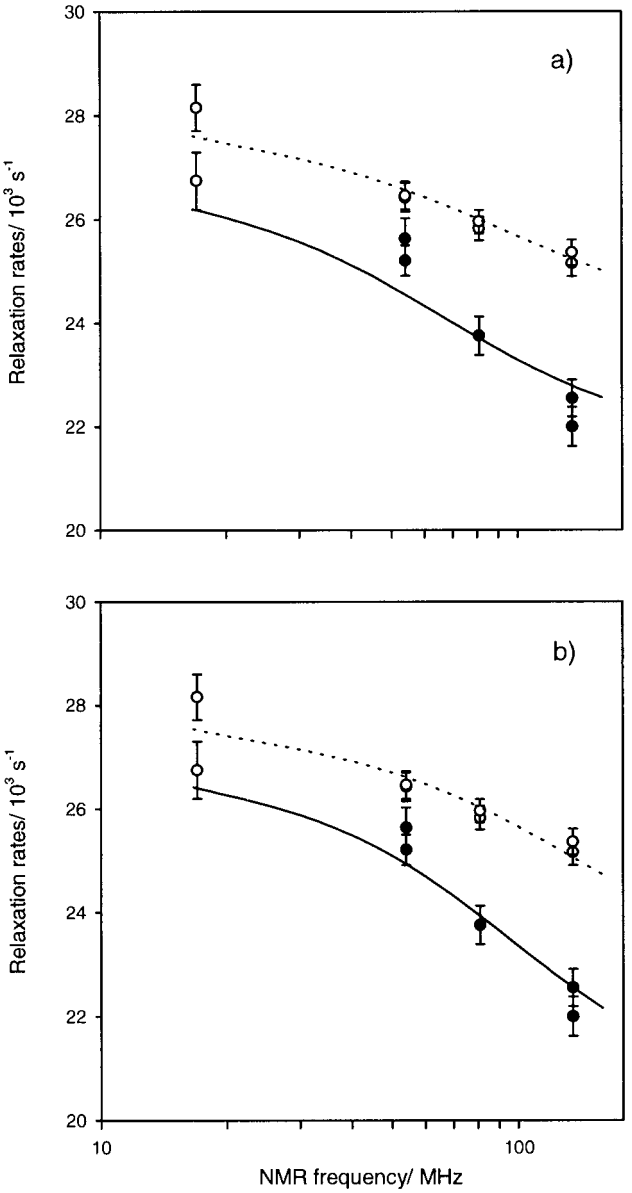

Figure 2. Frequency dependence of the ^{81}Br relaxation rates R_1^{eff} (full symbols) and R_2^{eff} (open symbols). The error bars, $\pm\sigma$, are the estimated experimental error. The two fits are performed under the assumptions of $\rho = 1.6$ (a) and $\rho = 1.4$ (b) axial ratios for the prolate micelles of $C_{16}TABr$ with r_{Br} set to 25.7 Å. The fitted micellar parameters are given in Table 1.

electromagnet (17 MHz). The inhomogeneous broadening of the ^{81}Br peak was negligible on all spectrometers ($\leq$10 Hz as determined from the ^1H spectrum of the same sample, $\leq$30 Hz for the lowest field).

The spin relaxation rates of ^{81}Br were showing a strong (about 5% per °C, comparable to our full effect; see Figure 2) temperature dependence. Therefore, great care has been taken to provide a stable and reproducible temperature during the experiments. Temperatures at the different spectrometers, set to 30 °C and controlled both at the beginning and at the end of measurements, were carefully (to within 0.1 K) calibrated together by using the temperature-dependent splitting of the ^2H NMR spectrum of C_6D_6 dissolved in a thermotropic liquid crystal.[27] Moreover, heating[28] caused by fast pulse repetition, essential to maximize the signal-to-noise ratio, was checked by isoconductive and identically sized samples of $K_3Co(CN)_6$ in water. Pulse repetition rates were then set slow enough to provide $\leq$0.1 K heating effect, as established from the highly temperature-sensitive ^{59}Co NMR spectrum.[29] Finally, the experimental errors indicated in Figure 2 include a $\pm$0.15 K estimated temperature error that accounts for both heating and setting uncertainties.

A spin relaxation study of ^{81}Br is complicated by the fact that ^{81}Br is an $I = {}^3/_2$ quadrupolar nucleus. In general, $I = {}^3/_2$ nuclei exhibit multiexponential transverse and longitudinal spin relaxation.[30,31] Moreover, the quadrupole coupling constant of ^{81}Br is very large and, therefore, the lines are very broad[25,32−35] when the electric field gradient at the nucleus is nonzero (Figure 1). This means that the spin relaxation *during* the applied rf pulses[36,37] is not necessarily negligible (in contrast, for example, to ^{23}Na), which virtually excludes using sophisticated multipulse experiments[38] and line shape analysis[39] for separating the components of the multiexponential relaxation. The observation, however, that the longitudinal and transverse relaxation rates (R_1^{eff} and R_2^{eff}, obtained as described below) of ^{81}Br in our sample are close to each other at all of our magnetic fields indicates that such experiments are not necessary and, in fact, are not even feasible. More importantly, the closeness of R_1^{eff} to R_2^{eff} implies that the three motional spectral densities, $J(0)$, $J(\omega_0)$, and $J(2\omega_0)$, that are included in the measured spin relaxation rates must also be close to each other. In other words, there is only a small relaxation dispersion step. Therefore, the relaxation decays are effectively single-exponential.[39,40] The case for a small relaxation dispersion is further supported by carefully[41] comparing the observed intensity of the ^{81}Br NMR signal in the micellar solution to the intensity one obtains in an aqueous NaBr solution (where extreme narrowing prevails for ^{81}Br and the line is more than 10 times narrower) of equal Br concentration. The intensities are equal to within 7%,[41] which shows that there is no undetected broad component of the Br signal in the studied micellar solution.

Since our relaxation times are about 40 μs, the ^{81}Br NMR signal is significantly influenced by the ringing (electronic and/or electroacoustic) of the probe[42,43] after the applied rf pulses. To reduce this effect, we applied a ringing reduction scheme[44,45] consisting of three closely spaced and phase-cycled rf pulses instead of a single rf pulse for recording the FID signal in the line width experiments. In the inversion recovery experiments we used the same composite pulse instead of the traditional detection pulse. Ideally, the three pulses in the composite pulse should be 90° ones and as short as possible. However, we judged it necessary (see below) to perform all experiments with the same pulse lengths and therefore with the same rf power level B_1. Hence, the rf field strength had to be adjusted to the weakest of that achievable without arcing on all spectrometers and probes of this study. This weakest B_1 field is $\gamma B_1 = 1.4 \times 10^5$ rad s^{-1}, which made the 90° pulses a bit too long (compared to the relaxation times). Therefore, three 70° pulses ($\sim$9 μs long each) were used instead in the composite pulse; this reduces somewhat (by $\sim$20%) the signal-to-noise ratio. Relaxation during the rf pulses[36,37] causes the inversion recovery experiment to be influenced by some systematic error. However, this error should be approximately second order in (τR_1^{eff}), where τ is the length of the 70° pulse, with the primary effect of mixing together $J(\omega_0)$ and $J(2\omega_0)$; the final effect is estimated to be smaller than the experimental errors in Figure 2.

The line width data R_2^{eff} are less sensitive to relaxation during the rf pulses. Their accuracy could instead decrease if some residual ringing penetrated our composite pulse. Such penetrating ringing was recorded without sample and was found negligible after a 20 μs (25 μs at the lowest field) acquisition delay following the composite pulse. To make sure that ringing

effects after 20 μs were negligible with the sample as well, we recorded FIDs not only on-resonance but also off-resonance[43] by setting either the frequency or (at the lowest field) the magnetic field off by about $\pm$30 kHz. Since the ringing pattern in relation to the signal varied a lot between those individual measurements while the fitted R_2^{eff} data were the same within the fitting error, we conclude that our line width data are not corrupted by ringing.

After these tedious (nevertheless essential to detect the small effect in Figure 2) considerations, the relaxation rates were obtained by fitting the FID and the "inversion recovery" data to single-exponential decays (a complex one for the FID, with also frequency and phase as free parameters). Since the inhomogeneous broadening of the ^{81}Br line is negligible, the FID provides the homogeneous line width. In the "inversion recovery" experiments, the fitted data points are the signal integrals that simplify (by canceling, in the short-pulse limit, any octupolar polarization effect[38,39,46]) the expression for the decay constant to that of eq 2. The final rate constants are

$$R_2^{\text{eff}} = \frac{J(0) + 2J(\omega_0) + J(2\omega_0)}{2} \tag{1}$$

for the transverse relaxation and

$$R_1^{\text{eff}} = \frac{2J(\omega_0) + 8J(2\omega_0)}{5} \tag{2}$$

for the longitudinal relaxation.

Results and Discussion

Recent small-angle neutron scattering experiments[47,48] refined the original picture[16,17] concerning the shape of C_{16}TABr micelles; it is now well established that (i) the growth of C_{16}TABr micelles starts at very low ($\leq$50 mM) surfactant concentrations and (ii) at around 100 mM (the concentration of the present study) the axial ratio ρ of the prolate aggregates is small, obtained as $\rho = 1.6$[47] or 1.3.[48] Moreover, analysis of accurate new field-dependent ^{2}H NMR relaxation data on C_{16}TABr-α-d_2[26] and reanalysis of a previous relaxation dispersion set,[49] in terms of spins diffusing over a prolate C_{16}TABr micelle,[50] support the scattering result of $\rho = 1.6$, whose value is then favored in the further analysis. We note that choosing a somewhat lower axial ratio does not change much our conclusions; to show this, we also provide the results obtained under the assumption of $\rho = 1.4$. Choosing an even smaller axial ratio (1.2) provides, besides a less credible fit for the ^{2}H relaxation data,[26] an unphysically fast (that is, faster than in infinitely dilute solutions of simple salts) diffusion coefficient of Br^- ions, while larger ($\geq$1.9) axial ratios are clearly inconsistent with the ^{2}H relaxation behavior.[26]

There are two dynamical processes that can significantly contribute to the spin relaxation of the Br^- ions (see Introduction) via modulation of the residual quadrupolar coupling χ_R left unaveraged by fast ($\leq$100 ps) molecular motions at the micelle$-$water interface. Since this residual coupling coincides with the surface normal, the translational motion of individual ions provides the first mechanism and micellar tumbling the second one. In principle, there are two diffusional modes that could contribute to relaxation: (i) lateral diffusion along the micellar surface and (ii) radial diffusion perpendicular to the micellar surface, i.e., the exchange of counterion between the regions perturbed and unperturbed by the micellar interface. This second mode, as has been shown earlier,[5$-$7,10] is rapid on the nanosecond time scale and provides, in the absence of added salt, a negligible contribution to spin relaxation. The principal reason is the high degree of counterion association to salt-free ionic micelles; for Br^- in C_{16}TABr solution it is around 0.8.[32,33,48,51] Moreover, the ion, which leaves the interface, rapidly re-enters there. Hence, on the nanosecond time scale the Br^- ions are effectively trapped by the electrostatic potential of the oppositely charged micellar surface. (In other words, the intermicellar exchange times are much longer than the correlation time for the motional averaging of the residual quadrupole coupling by lateral surface diffusion.) The predominance of lateral surface diffusion has been clearly indicated by ^{23}Na relaxation studies where frequency or orientation dependence of the relaxation rates convincingly followed the form predicted by the interface geometry.[9$-$11,52] The principal effect of radial diffusion is to set the value of χ_R; it becomes a population average of the values close to the headgroups and of zero outside the headgroup region. The picture above is, of course, an approximation that proved to be a judicious one.[9$-$11,52]

Hence, we model the motion of the Br^- ions, which leads through modulation of the residual quadrupole coupling to the observed quadrupole spin relaxation as surface diffusion on a rigid, freely tumbling prolate spheroid of axial ratio ρ. This process has been meticulously analyzed,[50] yielding a detailed recipe for numerically calculating the motional spectral density functions in the experimental relaxation rates in eqs 1 and 2. We note that the analysis proceeds essentially the same way for ^{2}H relaxation data on $C_{16}TA^+$ surfactant ions[26] and for ^{81}Br relaxation data on the counterions; a general assumption is that micellar tumbling, calculated from the Perrin equation,[50,53] is statistically independent from the lateral surface diffusion. Using the same dynamic model for analyzing the ^{81}Br data in the present work and the ^{2}H relaxation data of C_{16}TABr-α-d_2 obtained from in the same system[26] lends extra credibility to mobility differences of the Br^- and CTA^+ ions presented below.

Using the results of Halle[50] (see eq 7.3 there), we fit the experimental frequency-dependent relaxation rates as sums of spectral densities obtained for a given axial ratio ρ and expressed in the form of

$$J(\omega) = J_f + \frac{\pi^2}{5}\chi_R{}^2\, j_s(\omega;\tau_{\text{diff}},\rho) \tag{3}$$

for $I = {}^3/_2$ ($\chi_R = e^2qQ/h$, where eq_R is the residual electric field gradient[4] and the other symbols have their usual meaning[54]). Through this expression, three micellar parameters are obtained. First, the frequency-independent contribution to the spectral density functions J_f characterizes the time scale of the fast ($\leq$100 ps) averaging processes that reduce the quadrupole coupling constant from its instantaneous value to a residual one; this parameter is largely independent of the choice of the particular model for analyzing the frequency dependence of the relaxation rates. Second and third, the actual frequency dependence yields, through the model providing the reduced spectral density function $j_s(\omega;\tau_{\text{diff}},\rho)$,[50] the correlation time τ_{diff} and the residual quadrupole coupling χ_R. τ_{diff} characterizes the lateral surface diffusion, while χ_R contains information about the hydration of the counterion.

As a particularly important point, τ_{diff} is connected to the *angular* fluctuation caused by surface diffusion over a given curvature. To obtain the spatial lateral diffusion coefficient, D_{lat} requires the value of the minor semiaxis r of the prolate surface on which the spin-bearing particles diffuse. The defining equation is

$$D_{lat} = \frac{r^2}{\tau_{diff}} \quad (4)$$

By use of a frequently chosen way, supported in the present system by the results of the scattering experiments,[47,48] the minor semiaxis of a prolate micelle is estimated to be the all-trans length of the alkyl chain plus the headgroup diameter. In a previous ^2H NMR relaxation study, this radius has been set to 23.7 Å.[55] Nevertheless, the exact value remains somewhat disputable. To account for this uncertainty, we proceed with our present analysis, as in our related ^2H NMR study,[26] by setting the minor semiaxis to two separate values of 25.7 and 23.7 Å. Thus, it will be clearly demonstrated that this uncertainty has no major influence on the main conclusions of this paper. Poisson−Boltzmann calculations indicate that about 80% of the counterions are confined in a 5 Å vicinity to the headgroups. Hence, we assume (and use it in the analysis below) that r_{Br} is 2 Å larger than the corresponding micellar radius. A minor complication (discussed in detail in ref 26) arises from the fact that the micellar tumbling is defined by the hydrodynamic radius of the micelle that might be somewhat different from r_{Br}; for fast-diffusing particles, like the Br^- ion, the consequences are negligible.

The actual results of fitting the expression defined in eq 3 to our experimental data are presented in Figure 2a (for $\rho = 1.6$) and Figure 2b (for $\rho = 1.4$), while the corresponding sets of micellar parameters are collected in Table 1. Obviously, the parameter errors are large mostly because of the errors in the ^{81}Br relaxation rates, which are large compared to the (small) relaxation dispersion step. It is worth noting, however, that the actual experimental errors are a few percent, a rather good result delivered by our efforts documented in the Experimental Section. The surface diffusion coefficients, calculated from eq 4, are collected in Table 2, together with their counterparts for the surfactant ions.

In order of significance, the first result is that the Br^- ions are about 1 order of magnitude more mobile than the $C_{16}TA^+$ ions (Table 2). The D_{lat} of the $C_{16}TA^+$ surfactant ions has also been measured in spherical $C_{16}TACl$ micelles,[55] yielding low values (4.1×10^{-11} m^2/s) similar to those in Table 2. If nothing else, this finding obviously rules out binding or close association of the Br^- ion to specific sites at the headgroups on the ≥100 ps time scale. The uncertainty in our minor semiaxis and the axial ratio unfortunately causes the actual value of the spatial diffusion coefficient of Br^- to be less well defined, 81×10^{-11} m^2/s ≤ $D_{lat}(Br^-)$ ≤ 185×10^{-11} m^2/s. Thus, although the diffusion coefficient is somewhat reduced, we cannot say exactly how many times $D_{lat}(^{81}Br)$ is lower than the diffusion coefficient for the same ion at the same temperature in water at infinite dilution (225×10^{-11} m^2/s).[51]

The residual quadrupole coupling χ_R and the extreme narrowing contribution J_f to spin relaxation are complex functions of the interface structure and dynamics.[3] Therefore, the values obtained from the fit can perhaps be best used by comparing them to the corresponding quantities obtained for Na^+ ions in the vicinity of sodium bis(2-ethylhexyl) sulfosuccinate (AOT)[10] and sodium dodecyl sulfate (SDS)[12] headgroups. First, molecular dynamics simulation studies have convincingly shown that the dominant effect in establishing the rms instantaneous quadrupole coupling constant for ions in aqueous environment is the structure and fluctuations of the hydration shell.[3,56−58] In bulk, Br^- ions have an rms instantaneous coupling constant $\chi(Br^-)$ (derived from the experimental quadrupolar relaxation rates and the simulated correlation times[56]) that is about 10 times the same quantity $\chi(Na^+)$ for Na^+ ions. Scaling $\chi_R(Br^-)$ by the this factor and dividing it by the experimental Na^+ residual couplings found for AOT in the inverse hexagonal phase[10] and for SDS in the hexagonal phase[12] yield the Br^- order parameter $S(Br^-) = \chi_R(Br^-)/\chi(Br^-)$ relative to the Na^+ order parameter $S(Na^+) = \chi_R(Na^+)/\chi(Na^+)$. The ratio $S(Br^-)/S(Na^+)$ is ∼0.5 for AOT and ∼0.8 for SDS. As for a numerical estimate, assuming that the rms instantaneous coupling is about 30−70 MHz,[56] the order parameter $S(Br^-)$ comes to a low value of about 2−3%.

This low order parameter indicates that J_f is approximately proportional to the product of the square of $\chi(Br^-)$ and to the effective fast correlation time τ_f characterizing the (partial) averaging of $\chi(Br^-)$.[2,8] Thus, $J_f(Br^-)$ scaled down by 100 provides a comparison between the time scales of the fast fluctuation processes for Br^- and Na^+ ions. The obtained 100−110 s^{-1} [$=J_f(Br^-)/100$] falls closer to the $J_f(Na^+)$ in AOT (∼120 s^{-1}) than that in SDS (∼25 s^{-1}). Without simulation results at hand (except those for SDS[22]) it is difficult to speculate about the origin and significance of these differences. The actual numerical value of the effective fast correlation time, which is the time integral of the correlation function of the fluctuations of the instantaneous quadrupole coupling, comes to about 5−10 ps, an order of magnitude larger than that in dilute bulk solutions.[56]

TABLE 1: Four Sets of Micellar Parameters (See Text) Obtained in the Fits with Different Assumed Axial Ratios ρ and Radii r_{Br}[a]

	$\rho = 1.6$		$\rho = 1.4$	
	$r_{Br} = 25.7$ Å	$r_{Br} = 27.7$ Å	$r_{Br} = 25.7$ Å	$r_{Br} = 27.7$ Å
J_f (10^3 s^{-1})	10.9 ± 0.2	11.0 ± 0.2	10.2 ± 0.4	10.4 ± 0.3
χ_R (MHz)	0.97 ± 0.10	0.89 ± 0.09	1.28 ± 0.18	1.17 ± 0.15
τ_{diff} (ns)	6.5 ± 1.7	7.1 ± 1.9	4.9 ± 1.2	5.5 ± 1.3

[a] The fittings with $r_{Br} = 25.7$ Å are presented in Figure 2. The presented error bars correspond to $\pm\sigma$, where σ is the estimate of the random parameter error provided by the fitting using the Levenberg−Marquardt least-squares algorithm.[61]

TABLE 2: Lateral Diffusion Coefficients of the Br^- Counterions, Calculated from the τ_{diff} Values of Table 1 with the Help of Eq 4, and the Corresponding $C_{16}TA^+$ Surfactant Ions[26] Obtained from Fittings with Fixed Axial Ratios and Radii[a]

	D_{lat} (10^{-11} m^2/s)			
	$\rho = 1.6$		$\rho = 1.4$	
	$r_{Br} = 25.7$ Å	$r_{Br} = 27.7$ Å	$r_{Br} = 25.7$ Å	$r_{Br} = 27.7$ Å
Br^-	81−139	85−145	109−179	113−185
$C_{16}TA^+$	8.1−8.3	11.3−11.6	6.3−6.5	9.2−9.4

[a] Because of the asymmetric error region (see eq 4), the limiting values are given.

Conclusions

The most important result of this work is the fast, $\sim 10^{-9}$ m^2/s, surface diffusion coefficient of the Br^- ions. This value is somewhat reduced compared to that of the same ions in dilute bulk solutions; it is unclear how much of this reduction is coming from electrostatic attraction and from obstruction (by the protruding headgroups) effects. It might be indicative, however, that the same reduction factor is about 3 for Na^+ ions both with AOT[10] and with sulfate[12] headgroups. Moreover, neutron diffraction[59,60] and simulation[22,23] studies indicate a rather similar surface smoothness for aggregates with sulfate and trimethylammonium headgroups, and the simulated probability distribution functions for the headgroups and counterions show comparably small overlap in the two cases.

The most important reason for not being able to draw stronger conclusions is that *accurate* NMR relaxation studies of ^{81}Br in these (and presumably other[32−35]) micellar systems are rather difficult to perform. Most of the significant information is hidden in a small relaxation dispersion step (see Figure 2), which is only a couple of times larger than the best experimental error we could reach. (This is, to our knowledge, actually the first time that any frequency dependence for ^{81}Br relaxation is measured at all.) Nevertheless, the experimenter has no options; if we are interested in the behavior of Br^-, we cannot change the counterion to one that allows for easier NMR measurements. Despite all the errors, it is clear that the counterion diffuses much more quickly than the surfactant molecule so that those two cannot be closely associated on the $\geq$100 ps time scale. Additionally, the hydration structure and dynamics of the Br^- ion are fairly similar to that of the Na^+ ions in other micellar systems; the hydration shell of Br^- is less disturbed by the corresponding surfactant ion, as indicated by the smaller $S(Br^-)$.

As another aspect of this work, we found a dominant frequency-independent contribution to the ^{81}Br spin relaxation. This is connected to the low order parameter $S(Br^-)$ for the Br^- ion; the dispersion step is proportional to the square of this quantity. In our particular system, this means that the spin relaxation is less sensitive to global micellar parameters, such as micelle size and the surface diffusion coefficient of the counterion, while it is more sensitive to variation of the hydration structure and dynamics of the counterion on the 1−10 ps time scale. This feature commands caution when interpreting ^{81}Br relaxation data, recorded at one particular NMR frequency,[32−35] in terms of global micellar characteristics such as aggregate shape.

Acknowledgment. This work was supported by the Swedish Natural Science Research Council (NFR). N.H. thanks the Ernst Johnsson Foundation for a scholarship.

References and Notes

(1) Evans, D. F.; Wennerström, H. *The Colloidal Domain*; VCH Publishers: New York, 1994.
(2) Wennerström, H.; Lindblom, G.; Lindman, B. *Chem. Scr.* **1974**, *6*, 97.
(3) Linse, P.; Halle, B. *Mol. Phys.* **1989**, *67*, 537.
(4) Halle, B.; Wennerström, H. *J. Chem. Phys.* **1981**, *75*, 1928.
(5) Halle, B. *Mol. Phys.* **1984**, *53*, 1427.
(6) Halle, B. *Mol. Phys.* **1985**, *56*, 209.
(7) Halle, B. *Mol. Phys.* **1987**, *60*, 319.
(8) Halle, B.; Quist, P. O.; Furó, I. *Liq. Cryst.* **1993**, *14*, 227.
(9) Furó, I.; Halle, B. *Phys. Rev. E* **1995**, *51*, 466.
(10) Furó, I.; Halle, B.; Quist, P.-O.; Wong, T. C. *J. Phys. Chem.* **1990**, *94*, 2600.
(11) Quist, P.-O.; Blom, I.; Halle, B. *J. Magn. Reson.* **1992**, *100*, 267.
(12) Quist, P.-O.; Halle, B.; Furó, I. *J. Chem. Phys.* **1991**, *95*, 6945.
(13) Evans, D. F.; Mitchell, D. J.; Ninham, B. W. *J. Phys. Chem.* **1984**, *88*, 6344.
(14) Jönsson, B.; Wennerström, H. *J. Phys. Chem.* **1987**, *91*, 338.
(15) Hayter, J. B. *Langmuir* **1992**, *8*, 2873.
(16) Reiss-Husson, F.; Luzzati, V. *J. Phys. Chem.* **1964**, *68*, 3504.
(17) Ekwall, P.; Mandell, L.; Solyom, P. *J. Colloid Interface Sci.* **1971**, *35*, 519.
(18) Lu, J. R.; Simister, E. A.; Thomas, R. K.; Penfold, J. *J. Phys. Chem.* **1993**, *97*, 6024.
(19) Su, T. J.; Lu, J. R.; Thomas, R. K.; Penfold, J. *J. Phys. Chem. B* **1997**, *101*, 937.
(20) Magid, L. J.; Han, Z.; Warr, G. G.; Cassidy, M. A.; Butler, P. D.; Hamilton, W. A. *J. Phys. Chem. B* **1997**, *101*, 7919.
(21) Ilekti, P.; Picullel, L.; Tournilhac, F.; Cabane, B. *J. Phys. Chem. B* **1998**, *102*, 344.
(22) MacKerell, A. D. *J. Phys. Chem.* **1995**, *99*, 1846.
(23) Böcker, J.; Brickman, J.; Bopp, P. *J. Phys. Chem.* **1994**, *98*, 712.
(24) Kuhn, H.; Rehage, H. *Ber. Bunsen-Ges. Phys. Chem.* **1997**, *101*, 1493.
(25) Firouzi, A.; Atef, F.; Oertli, A. G.; Stucky, G. D.; Chmelka, B. F. *J. Am. Chem. Soc.* **1997**, *119*, 3596.
(26) Hedin, N.; Sitnikov, R.; Furó, I.; Henriksson, U.; Regev, O. *J. Phys. Chem. B* **1999**, *103*, 9631.
(27) Farrant, R. D.; Lindon, J. C. *Magn. Reson. Chem.* **1994**, *32*, 231.
(28) Hoult, D. I.; Lauterbur, P. C. *J. Magn. Reson.* **1979**, *34*, 425.
(29) Levy, G. C.; Bailey, J. T.; Wright, D. A. *J. Magn. Reson.* **1980**, *37*, 353.
(30) Hubbard, P. S. *Phys. Rev.* **1969**, *180*, 319.
(31) Werbelow, L. G. In *Encyclopedia of Nuclear Magnetic Resonance*; Grant, D. M., Harris, R. K., Eds.; Wiley: Chichester, 1997; Vol. 6, p 4092.
(32) Lindblom, G.; Lindman, B.; Mandell, L. *J. Colloid Interface Sci.* **1970**, *34*, 262.
(33) Lindblom, G.; Lindman, B. *J. Phys. Chem.* **1973**, *77*, 2531.
(34) Lindblom, G.; Lindman, B.; Mandell, L. *J. Colloid Interface Sci.* **1973**, *42*, 400.
(35) Caboi, F.; Monduzzi, M. *Langmuir* **1996**, *12*, 3548.
(36) Maarel, J. R. C. v. d. *J. Chem. Phys.* **1989**, *91*, 1446.
(37) Maarel, J. R. C. v. d.; Tromp, R. H.; Leyte, J. C.; Hollander, J. G.; Erkelens, C. *Chem. Phys. Lett.* **1990**, *169*, 585.
(38) Jaccard, G.; Wimperis, S.; Bodenhausen, G. *J. Chem. Phys.* **1986**, *85*, 6282.
(39) Kenéz, P. H.; Carlström, G.; Furó, I.; Halle, B. *J. Phys. Chem.* **1992**, *96*, 9524.
(40) Halle, B.; Wennerström, H. *J. Magn. Reson.* **1981**, *44*, 89.
(41) Hedin, N.; Furó, I. *J. Magn. Reson.* **1999**, 141.
(42) Fukushima, E.; Roeder, S. B. W. *Experimental Pulse NMR*; Addison-Wesley: Reading, MA, 1981.
(43) Gerothanassis, I. P. *Prog. Nucl. Magn. Reson. Spectrosc.* **1987**, *19*, 267.
(44) Zhang, S.; Wu, X.; Mehring, M. *Chem. Phys. Lett.* **1990**, *173*, 481.
(45) Zhang, W.; Furó, I. *Biopolymers* **1993**, *33*, 1709.
(46) Werbelow, L. G. *J. Magn. Reson.* **1983**, *52*, 282.
(47) Berr, S.; Jones, R. R. M.; Johnson, J. S. *J. Phys. Chem.* **1992**, *96*, 5611.
(48) Quirion, F.; Magid, L. J. *J. Phys. Chem.* **1986**, *90*, 5435.
(49) Törnblom, M.; Henriksson, U.; Ginley, M. *J. Phys. Chem.* **1994**, *98*, 7041.
(50) Halle, B. *J. Chem. Phys.* **1991**, *94*, 3150.
(51) Fabre, H.; Kamenka, N.; Khan, A.; Lindblom, G.; Lindman, B.; Tiddy, G. J. T. *J. Phys. Chem.* **1980**, *84*, 3428.
(52) Quist, P. O.; Halle, B. *Phys. Rev. E* **1993**, *47*, 3374.
(53) Perrin, F. *J. Phys. Radium* **1934**, *5*, 497.
(54) Abragam, A. *The Principles of Nuclear Magnetism*; Clarendon: Oxford, 1961.
(55) Söderman, O.; Henriksson, U.; Olsson, U. *J. Phys. Chem.* **1987**, *91*, 116.
(56) Roberts, J. E.; Schnitker, J. *J. Phys. Chem.* **1993**, *97*, 5410.
(57) Engström, S.; Jönsson, B.; Jönsson, B. *J. Magn. Reson.* **1982**, *50*, 1.
(58) Chen, S. W.; Rossky, P. J. *J. Phys. Chem.* **1993**, *97*, 10803.
(59) Cabane, B.; Duplessix, R.; Zemb, T. *J. Phys. (Paris)* **1985**, *46*, 2161.
(60) Tabony, J. *Mol. Phys.* **1984**, *51*, 975.
(61) Press, W. H.; Flannery, B. P.; Teulolsky, S. A.; Vetterling, W. T. *Numerical Recipes*; Cambridge University Press: Cambridge, 1986.